

A Predictive Approach to Estimating Build Time and Material Usage Through an Intuitive Design for Additive Manufacturing Score

Ryan Delaney¹, Catherine B. Ashley², Andrew Killian², Nicholas Meisel^{*3}

* Corresponding Author: nam20@psu.edu

¹ Department of Mechanical Engineering, The Pennsylvania State University, University Park, PA 16802

² CRG Defense, Miamisburg, OH 45342

³ School of Engineering Design and Innovation, The Pennsylvania State University, University Park, PA 16802

Abstract

Reliable material estimation and print time models are essential to guide decisions throughout early product development in additive manufacturing (AM). Material and time can easily be found from slicing a STL file; however, if only early design concepts, or legacy drawing files are available, an alternative method is needed. Ideally, preliminary estimation models can be used to provide quick insight into print feasibility, efficiency, and budget constraints before moving to CAD modeling. Failure to perform early-stage analysis can lead to parts with extensive print times, inflated costs, and material waste. This paper explores the use of a scoring worksheet to aid in evaluating drawing files for both laser powder bed fusion and material extrusion processes. The resulting score, which acts as a rapid, intuitive measure of a part's suitability for AM, is implemented inside a material- and time-estimation model derived only from parameters obtainable from two-dimensional drawing files. The estimations are then compared to actual three-dimensional, CAD-based slicing data from printing software.

1. Introduction

Additive manufacturing (AM) is becoming an increasingly used tool in manufacturing settings, as industries find alternative methods to traditional manufacturing. Buyers are looking for customizable, innovative, and high-quality parts, with simultaneously reducing manufacturing cost and lead times [1]. Due to AM's ability to produce high shape complexity parts at a fraction of the weight of traditionally manufacturable designs, low production costs can be achieved through savings in material costs, energy consumption and short cycle times. It is essential to accurately estimate cost during the initial phase of design, as cost quotations are used daily by designers when building prototypes or designing parts [2]. Because production costs vary from operation to operation – each accounting for different internal factors – early cost estimation can be challenging to predict. However, build time and material usage are more universally comparable across each practice, making them a reliable target for early estimates. Regardless of which parameters are used in their calculations, all estimators start from the same source: a 3D file – typically in .STL format – which help define a parts actual geometry including volume, height and surface area. By extracting print parameters from a 2D-drawing file or sketch, it becomes possible to estimate build time and material usage earlier in the design phase, inherently saving cost and time down the line when it comes time to manufacture and produce. Due to the extensive time, expertise and resources it takes to generate a CAD model, it is not always practical when trying to get an early estimate of

build time and material usage. In the case of legacy drawings, where digital representation is absent, producing CAD solely for estimation can be inefficient. A method that enables estimates without requiring full CAD data can streamline the evaluation process and accelerate decision-making for AM parts.

However, even though AM estimators continue to grow quickly, they still face issues regarding model and feature classification. Prior to estimating a part's cost, material usage, and build time, it may undergo screening, ranking and support information [3]. An in-depth exploration in shape geometry, material selection and assembly requirements can provide the necessary information needed for estimator inputs. Some cost models approach the final cost as the sum of all resources it consumes, including materials, capital, build time, energy, and information, with other models incorporating post-processing and labor as well [4]. These models will leverage all available information, in hopes of achieving a more accurate estimation. However, if these estimates are needed early in the design process, few such parameters may be available. Evaluating a part's suitability for AM and generating accurate estimates require close collaboration between experts in design for additive manufacturing (DfAM) working to achieve a scoring rubric and estimator that (1) accurately represents a part's printability and (2) provides close approximates to the true value.

This paper takes the first steps in implementing an intuitive DfAM scoring approach, obtained from evaluating a parts 2D drawing file, inside of an estimation model to accurately predict a part's total build time and material usage. Specifically, it shows how parts of varying geometric features, bounding box volumes and process selection can come together in a way to estimate material volume and time, without the need of a 3D CAD part or STL file. This provides a new avenue in AM to help address limitations in industry, particularly the significant time investment needed to produce CAD models solely for initial suitability assessments, and initial "gut checks" of parts for AM during the preliminary design phase.

2. Background

The ability to understand which parameters to include in a material usage and time estimation model relies on (1) the understanding of a part's printability, (2) which features affect that printability, and (3) how additive manufacturing has been used to evaluate and score parts previously. With this information in mind, such parameters can be carefully selected, evaluated within a scoring metric, and implemented inside a cost and build model.

2.1. Additive Manufacturing Part Evaluation

From manufacturing process considerations including part orientation [5–8], post processing and support removal [4,9,10], to geometric considerations fillet guidelines, overhangs, and bridge features [11,12], there are several key principles to consider when it comes to designing for AM. Using the guidelines from researchers, as well as their own expertise in AM, original equipment manufacturers (OEMs) such as FormLabs [13], Stratasys [14] and ProtoLabs [15] created their own generic guidelines for certain machines and processes, with other AM suppliers and contributors as well [11,16]. From such guidelines, both quantitative and qualitative metrics can be generated to assess how well a part is designed for AM.

Although many design guidelines for AM exist, there remains a need for evaluation that employs these guidelines to help inform decisions such as manufacturability, material usage or print time early in the design process. Booth et al. developed a worksheet which asks simple questions about components – aimed at assisting novices when designing for material extrusion (MEX) [5]. This scoring worksheet takes a qualitative approach to scoring, asking the user about the types of features that are included in the design, rather than focusing on the specific dimensions of the features. Bracken et al. established a similar worksheet, but take a more quantitative approach, identifying specific geometric dimensions that influence a parts suitability for metal powder bed fusion [17]. Ultimately, Bracken et al.’s Geometric for Additive Part Selection (GAPS) worksheet focuses on nine key features for laser powder bed fusion (LPBF) and ranks them on a three-tier scale depending on the dimensions of these features as found in the evaluated design. Both Booth et al. and Bracken et al. worksheets provide a final score which directly correlates to the printability of one’s part.

While manual scoring worksheets offer an organized way to assess printability, more recent approaches leverage data-driven methods to automate and potentially improve part selection decisions. Yang et al. introduced a cloud-based tool to analyze CAD models, extract their geometric features and output predicted potentials of that part in five fields; economics, customization, light-weighting, part consolidation and internal channels [18]. Using machine learning (ML) and a sample size of 1000 parts, the dataset was examined similarly to what was demonstrated with Li et al. [19]; a learning-based algorithm to accurately capture desired parameters and minimize error. Machine learning’s increasing popularity can be attributed to the ability to minimize or eliminate the need for human input and therefore reduce potential human biases among the data [20]. Page et al. likewise used six ML algorithms to locate AM part candidates, each taking different approaches to part selection. By inputting a part into each ML algorithm, seven metrics are outputted as percentages: potential for (1) lightweighting, (2) customization, (3) internal channels/structures, (4) part consolidation, (5) designed surface structures, (6) specific material options and finally economic feasibility. Although many AM part evaluation methods focus on assessing printability using 3D CAD models and assume economic feasibility, accurately estimating built time and material usage remains a necessity for informed part selection. Research has introduced various models to quantify these aspects and support more comprehensive assessments of AM processes.

2.2. Cost and Time Models for Additively Manufactured Processes

Over the years, AM cost and time modeling have continued to evolve, with an increase of new models, frameworks, and estimators. Broadly speaking, estimators can be classified as either product-orientated and process-orientated [21]. Product-orientated estimation focuses on the comparing new parts to the history of previous manufactured products, while process-orientated estimation focuses on a part’s geometric features and the necessary manufacturing operations to produce them. Using a hierarchical classification model, the two main categories for cost-estimation are quantitative and qualitative, with the four subcategories being intuitive, analogical, parametric and analytical. [22–24]. Qualitative techniques are best for early design stages as they require little detailed information. This technique focuses on incorporating previous part history data and feature similarities into the new part to save on computation time. Quantitative techniques are more accurate however, as they solely rely on product design and dimensions, where the data is input into an analytical function to calculate time and cost. Kadir et al. discuss the classifications based

on different perspectives. Finance and accounting may take a more method-based approach while manufacturing may take a more task-based approach.[25].

Qualitative models are often represented using geometric properties, such as bounding box volume, and approximate volume [26]. Additionally, the chosen AM process type used for estimation can dictate which machine properties must be used. For example, laser scanning processes (LSP) such as powder bed fusion (PBF) and stereolithography (SLA), will often account for process parameters such as scanning power, velocity, layer thickness, path, etc. in the model [21,25–29]. For MEX estimation models, scanning speed is replaced by nozzle speed, and the most commonly referenced additional parameters include nozzle size properties, layer thickness and infill density [26,30–32]. Ruffo et al. previously developed a model to accurately predict time for parts manufactured using laser sintering. For their model, the only input parameters consisted of volume, surface area, height, and bounding box volume. From these input parameters, the following three estimations were computed and output: (1) recoating time, (2) scanning time, and (3) pre- and post-processing time [27]. These three times were summed to find the total print time of each part and compared to the real print times. From the study, it was found that there was a slight underestimation in scanning time, which was balanced by an overestimate in recoating time. The overall time model was found to overestimate the real production time, with a maximum total error of real time of 13%.

Campbell et al. identified an alternate approach to estimating build time using information found within 2D drawing files, as opposed to importing 3D CAD Files [2]. This model was developed for SLA and used basic shapes alongside their respective volumetric calculations to determine the overall part volume, with assistance from TK Solver, a mathematical problem-solving software. The results showed a percentage error between 12.75% to 6.78%, with the high percentage errors belonging to parts made up of more geometrically complex shapes. However, printing in a non-ideal print orientation can increase the amount of material waste and supports required, increasing both the print time, and time to post-processing [6,8]. Alexander et al. performed a study for both fused deposition modeling (FDM) and SLA, which not only estimated cost and time, but also how different orientations affect these two [7]. Parts with higher accuracy consist of larger print costs and longer build times, with orientation slightly affecting each study.

Alternatively, Simpson proposed a simplified cost and time model for metal single laser powder bed fusion [33]. His approach breaks the cost equation into machine related costs, material related costs and post-processing related costs, while the time model requires part volume, build rate, layer height, maximum part height and recoat time. Simpson discusses that geometric features such as overhangs supports, build orientation and other print characteristics such as spatter, electricity usage, powder recycling to name a few can complicate each model. By eliminating these specific elements from the estimation approach, it makes it more feasible for use if there is no CAD model available yet. However, with one of the key inputs being part volume, it can be quite difficult to calculate the volume of a complex, freeform part if no CAD model has yet been developed for a part being estimated. While estimators which use CAD models generally provide greater accuracy over those without, due to them providing geometric dimensions, the challenge in estimating material usage and time comes down to technique selection and which factors to include.

3. Manufacturability Scoring and Part Estimation Framework

Despite the progress made with CAD-driven evaluation techniques and estimation methods, limited attention has been given to techniques and estimators that rely on 2D drawings. This section explores the criteria required to estimate the material usage, and build time needed for AM analysis, starting with the need for a unique scoring template suitable for use with both LPBF and MEX processes. The general scoring worksheet solely relies on features and information only found in 2D drawing files, with no expectation of a completed CAD file. The worksheet will establish acceptance criteria, common geometric features and training on how to score potential printable parts using only part drawings and initial design schematics. The information extracted from the scoring templates is then used in the proposed material usage and build time models to accurately estimate these two desired outputs. The section is separated into two specific phases: the DfAM scoring approach (Section 3.1) and the predictive model for both material usage and build time (Section 3.2), with each section discussing the different approaches for both LPBF and MEX.

3.1. DfAM Scoring Approach

While preparing a scoring worksheet for AM, the most common geometric features affecting AM capabilities were sought. Using a dataset of 50 randomly selected parts from the 2019 ABC dataset, each part was evaluated by recording all geometric features, along with noting similarities between features across different parts.[34]. Parameters that will influence whether a part can be printed or not can be categorized into three main categories. The first includes features where larger dimensions are more desirable and improve print success. These features are outlined in the first section of Figure 1, and include larger pin/cylinder diameters, thicker walls, wider grooves, more generous fillets, and gently inclined surfaces, all essential to prevent structural failure whilst printing. The second category, outlined in the second section of Figure 1, involves features where smaller dimensions are more beneficial. These include shorter horizontal overhangs and bridges, smaller horizontal internal holes, lesser height/width ratios and thinner, thick sections. These are utilized to minimize the need for support material. Lastly, the third category consists of features that require explicit design checks, such as verifying the presence of escape holes, and ensuring all threaded features are accounted for. These are depicted in the third and final section of Figure 1.

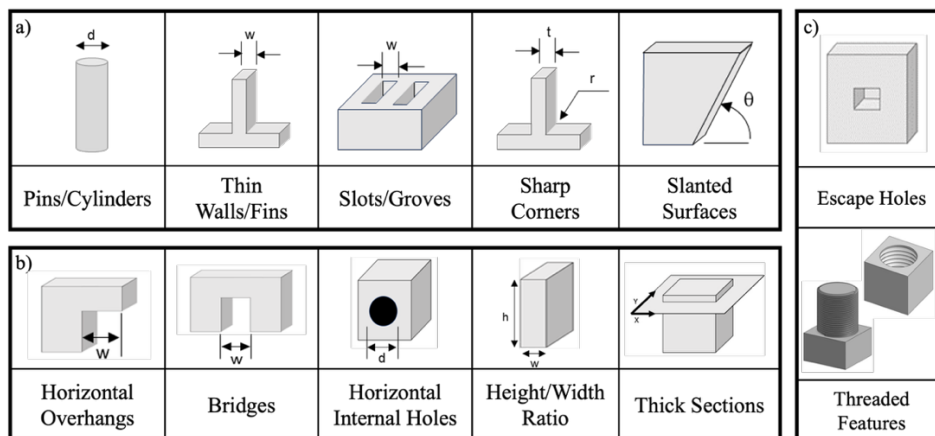


Figure 1. Common Geometric Features : a) Larger Features Desirable, b) Smaller Features Desirable, c) Explicitly Checked Features.

The initial scoring rubric adapted the three-tier scoring structure demonstrated in the GAPS worksheet from Bracken et al., however, after extensive testing on a subset of 50 randomly selected parts from the 2019 ABC dataset, it was concluded that a wider range of scoring was needed to see variations in data [34]. A majority of parts that were scored with the three-tier rubric received the highest score for several categories, resulting in a top-heavy distribution that skewed both the individual part DfAM score and the nominal DfAM score, which is an average of all DfAM scores in the dataset. The rubric was increased to five categories to remove the top-heavy distribution and achieve a more accurate individual and nominal DfAM score. The scoring rubrics can be seen in Figure 2, which shows the change in tier levels due to top-heavy distribution. The scoring metric was created into 12 categories, with five scoring tiers for all processes except height/width ratio, thick section and threaded feature position, which only include three tiers. [5,15,17,35–41]. The five different tiers highlight the candidacy of printing with AM: the bottom tier indicating dimensions which will lead to print failures, while higher tiers indicate increasing likelihoods of successful prints.

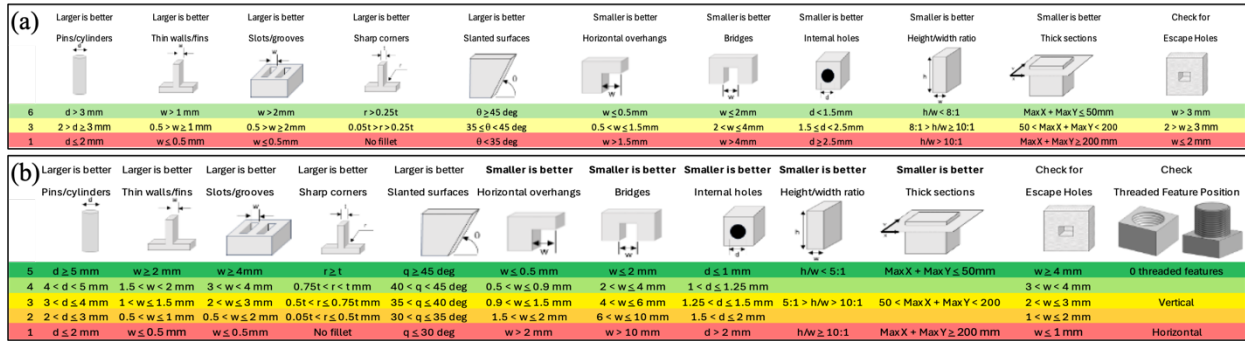


Figure 2. Comparison of scoring rubrics: (a) 3-tier rubric adapted from GAPS worksheet, (b) updated 5-tier rubric.

With the three sections containing the most prevalent geometries seen on parts destined to be printed with AM, a scoring criterion was needed to account for dimensional variations. The threshold of feature print success significantly changes depending on the additive process, such as LPBF or MEX, as well as the type and brand of machine being printed on. For MEX, the guidelines were obtained from popular OEMs and specific machine-based data analyzed from existing ‘torture test’ prints, [5,15,37,39,41], whereas for LPBF, the GAPS research paper by Bracken et al, and various data-driven guidelines were used [11,17,36]. For categories where larger features are more desirable, minimum values was set as the middle tier, as anything greater than this value would score higher and therefore be more desirable for printing. Conversely, for categories where smaller features are more beneficial, the maximum value was set to the bottom tier, representing the worst case scenario. Values smaller than this threshold are more desirable for printing and will receive higher scores. Each worksheet contains the same scoring criteria, however the threshold and ranges for scores varies based on process. The most significant difference between each process lies in the escape holes section. Escape holes are a requirement for LPBF, but not necessary for MEX. If a part lacks escape holes and is intended for LPBF, then the part will score a 1 for this category. If the part is being printed using MEX, it may receive a higher score, depending on the extent of its hollowness, since escape holes are not a requirement for this process.

To evaluate a part's additive manufacturability, an interactive scoring worksheet was created to aid in confirming the printability of various parts. The worksheet includes (1) the scoring criteria outlined in Figure 3, (2) a generalized note on how to score the parts, and (3) orientation notes regarding the drawing views. The worksheet is expressed with a parts 2D orthographic projections with all relevant dimensions which are used for scoring. Instead of solely including a typical isometric view in the drawing, the worksheets can alternatively include a 3D model of the CAD part, if available. This 3D model, embedded into the PDF worksheet, allows the viewer to rotate around the part to check for undefined features that may not be explicitly shown or easily interpreted in the orthogonal projections. The full worksheet with the embedded 2D drawing is shown in Figure 3.

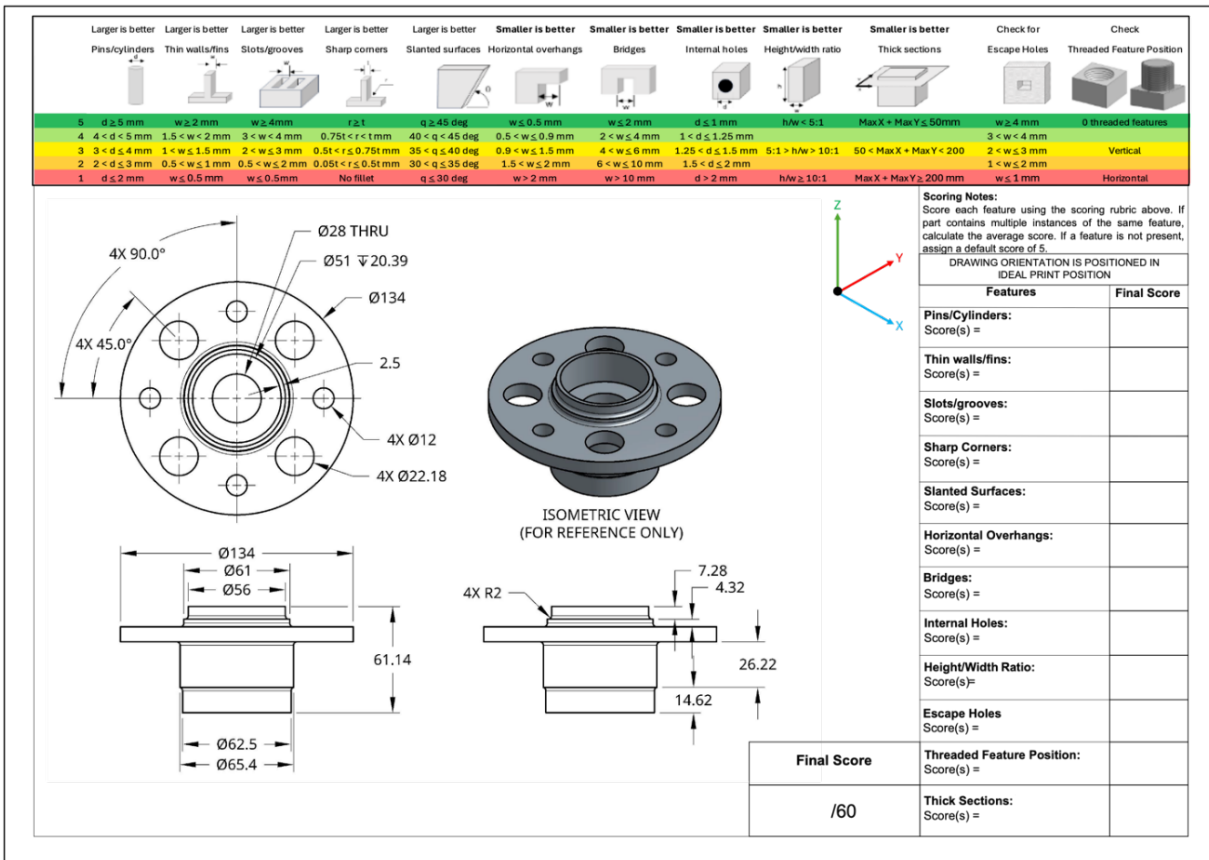


Figure 3. MEX Scoring Worksheet with 2D Drawing

It is important to note that there is one crucial assumption that drives not only the scoring worksheet, but also the estimators, which is the part orientation. To demonstrate the accuracy of the assessment and modeling approach, as well as maintain consistency across each drawing, the orientation is considered fixed, meaning there has been no orientation manipulation when scoring. The authors acknowledge that a drawing's orientation may not be the most ideal print orientation for a given part, especially when considering legacy designs, and that is approach is unlikely when leveraging the sheet in-practice. [8]. Part orientation plays a key role in support generation, surface quality, and overall print success. A design that is unprintable in one orientation may become feasible—or even optimal—in another, however, when evaluating parts using 2D drawings, interpretation is left to the scorer, which can lead to inconsistent orientations of the same part. Different

scorers may visualize the part from different perspectives, making it difficult to evaluate the drawings accurately, especially since 2D views are fixed. To minimize bias and maintain consistency across the evaluation process, the assumption that the drawing orientation was the print orientation was noted on the worksheet itself, as without it, different evaluators may try to re-orient the part and score it differently

After the user examines each category for a given drawing, they then input the scores for each feature category as applicable to the drawing being evaluated. To determine the score for each category of a given part, the features are found and highlighted within the drawing. If a part contains only one of the features from the scoring rubric, it is given the appropriate score for that single feature. However, if a part contains multiple of that feature, such as multiple fillets or bridges with varying dimensions, each feature is scored individually and then averaged to determine the final score for that category. The final values for the 12 categories are input into the worksheet, where the final DfAM score is automatically summed and displayed for a given part. While this final DfAM score is primarily used as an input parameter for later estimation of material usage, and build time, it can also serve as an indicator of the manufacturability of a given part. This is especially relevant when assessing legacy designs for their suitability for manufacturing with modern AM technology.

3.2. Predictive Model for Build Time and Material Usage

Using the score from the respective worksheet, an estimator was built to calculate the build time and material usage for both LPBF and MEX processes. Due to the different print parameters found within each process, such as LPBF needing laser scan time, recoating time, and pre-/post-processing time [27], and MEX applications needing process specific parameters such as nozzle diameter, different models were developed for each process type. Section 3.2.1 highlights the background behind the MEX build time and material estimator, whereas section 3.2.2 highlights the LPBF processes and its own build time and material estimator.

3.2.1. MEX estimator

Due to this estimator being used for early designs, before 3D CAD files may be available for slicing and estimation, the parameters used in the estimator need to be those that can be extracted from 2D drawing files. Volume can be approximated several ways, with one way including estimating basic shapes of the part and summing the estimated volumes [2] or using the maximum length, width, and height dimensions to find the part's bounding box volume. Due to the complexity of some parts, estimating volume based on the summation of basic shapes would be too difficult and time consuming to be beneficial in early design. For the analysis in our proposed approach, the maximum bounding box dimensions are instead used to calculate the bounding box volume. The maximum dimension in the z-direction of a 2D drawing is taken to be the maximum height, which was used to determine the number of layers for a part. The number of layers, L , is found in Equation 1, where h refers to the layer height and z refers to the maximum height in the z-direction.

$$L = \text{Round} \left(\frac{1000z}{h}, 0 \right) \quad (1)$$

The layer delay time indicates the total time duration required for the machine to move vertically from one layer to the next, with the delay time affecting the bonding between layers and

dimensional accuracy [42]. The greater the height of a part, the more layers that part contains, and therefore a higher layer delay time, indicating more time required for taller prints. The layer delay time, t_L , is found in Equation 2, where t_d , refers to the machine delay time per layer, and is often a constant variable and varies depending on the machine. The value of 1.145 was determined from calibrating and iterative tuning of the time model. The model predictions were compared to actual outcomes and adjusted accordingly to achieve the highest accuracy and minimize estimation error.

$$t_L = \frac{t_d L^{1.145}}{3600} \quad (2)$$

Using the DfAM score from the scoring worksheet, a correction factor can be found, which is the ratio of a part's individual DfAM score to the dataset's nominal DfAM score. As the dataset grows in size, the nominal DfAM score changes to account for the additional parts. This correction factor is meant to help identify how one individual design is compared against the rest of the evaluated population, which then helps us with later calculations for time and material usage. This correction factor is believed to help increase build time and material usage accuracy as more parts are added to the dataset. The correction factor, C is found in Equation 3, where s refers to the scores, and the superscripts DfAM and nom refer to individual DfAM score and nominal DfAM score, respectively.

$$C = \frac{S_{DfAM}}{S_{nom}} \quad (3)$$

This estimator aims to predict the part volume from the bounding box volume and the volume of support required per part. The DfAM score is based off of geometric features which often require support material, so this score, alongside the correction factor are used to estimate the part volume, support volume, and total volume, which is the summation of the two. The part volume, V_p , is given by Equation 4, support volume, V_s , by Equation 5 and total volume, V_t , by Equation 6, where V_{bb} refers to the bounding box volume. The value of 1.85 was determined from iterating estimated values of volume. The volume predictions were compared to actual outcomes and adjusted accordingly to achieve the highest accuracy of both part and support volume.

$$V_p = \frac{V_{bb}}{(S_{DfAM} + S_{nom})^2 (1 + C)^c} \quad (4)$$

$$V_s = \frac{V_p}{S_{DfAM} (1 + C)^{1.85}} \quad (5)$$

$$V_t = V_p + V_s \quad (6)$$

The support material is not printed at the same rate as the normal material for the part, therefore print time also needs to be broken into two pieces, support time and build time. To calculate both times, the amount of pre/post-processing needs to be estimated first. The pre/post processing required, P , is given by Equation 7, where $P_{pre/post}$ refers to the average pre/post-processing percentage required for an overall part and P_{pre} and P_{post} refer to the average additional

percentage of pre-/post-processing that may be required depending on a part's size, shape or orientation [43].

$$P = (P_{pre} + P_{post}) + (s_{nom} - s_{DfAM})P_{\frac{pre}{post}} \quad (7)$$

The support time considers printer capabilities to print supports, as well as the percentage of pre-/post-processing required. Build time also considers the percentage of pre-/post-processing required and solely focuses on the print time of the part volume. The support time, t_s , is given by Equation 8, and build time, $t_{b,MEX}$, is given by Equation 9, where P refers to the pre-/post processing required, \dot{V} refers to the volumetric build rate, N refers to the nozzle diameter, and v_s refers to the support print speed. Similarly to the delay time equation, the values of 1.1 and 1.7 were determined from iterative tuning of the time model. The predictions were compared to actual time values, and constants were incorporated to achieve a higher-level accuracy for both support and build time for MEX processes. The total build time, t_{bld} , is the summation of layer delay time, support time and build time per part.

$$t_s = \frac{V_s}{(3.6Nv_s h)}(1 - P)1.7C \quad (8)$$

$$t_{b,MEX} = \frac{V_p}{(3600\dot{V})}(1 - P)1.1C \quad (9)$$

$$t_{bld,MEX} = t_L + t_s + t_{b,MEX} \quad (10)$$

3.2.2. LPBF Estimator

The LPBF build time and material usage estimator follow the same initial steps as the MEX estimator, however, instead of calculating layer delay time, recoat time is used. Recoat time refers to the amount of time needed for the machine to deposit a new layer of powder [29], and is given by Equation 11, where t_r refers to the total recoat time per part and t_R refers to the amount of time a machine takes to recoat each layer, often a constant variable and varies depending on the machine.

$$t_r = \frac{t_R L}{3600} \quad (11)$$

Determining the part volume and support volume are found the same way as expressed in Equation 4 and Equation 5. The next change between the processes is the formula for calculating the amount of time to scan support material, as well as the amount of time to build solely the part. For the support scan time, t_{scan} , given by Equation 12, can be determined using the velocity scan speed, v_{ss} , laser focus diameter, d_{focus} , the layer height, h , and nominal DfAM score, s_{nom} . The build time for a given part using LPBF, denoted $t_{b,LPBF}$, is then given by Equation 13.

$$t_{scan} = \frac{V_s}{3.6d_{focus}hv_{ss}s_{nom}} \quad (12)$$

$$t_{b,LPBF} = \frac{V_P}{3600\dot{V}}(1 - P)S_{DfAM}C \quad (13)$$

$$t_{bld,LPBF} = t_r + t_{scan} + t_{b,LPBF} \quad (14)$$

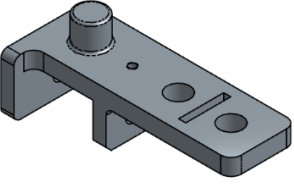
4. Case Studies

To demonstrate the use of the scoring worksheet and estimators detailed in Section 3, two case studies are presented. These case studies were selected to represent contrasting scenarios: one that appears intuitively well-designed for AM, and one that is not. Both parts were selected from the 50 set of parts obtained from the 2019 ABC dataset and chosen to represent extremes in the data [34]. For each case study, the same part is analyzed for both MEX and LPBF.

4.1 Case Study 1

The first case study follows the scoring and estimation of the part denoted as 000. The parts dimensions and bounding box volume can be seen in Table 2, alongside its isometric view for illustrative purposes; as discussed previously, a 3D CAD model is not necessary to execute the scoring and estimation approach in this work. Intuitively, this part is not ideal for either AM process, due to its wide and flat geometry all around, lead to warping or layer adhesion issues during printing. These large bridge and overhang sections will also require more material usage and increase the total build time. With the previously discussed assumption that the build orientation is fixed to that of the drawing, the orientation of the part cannot be altered to find an alternative print orientation, even though it may be beneficial.

Table 1. Part 000 Maximum Dimensions

	Drawing Dimensions	Value
	Maximum X [mm]	203.2
	Maximum Y [mm]	82.55
	Maximum Z [mm]	78.98
	Bounding Box Volume [mm ³]	274662.12

4.1.1. Scoring Rubric of Case Study 1

Using only the 2D drawing information to determine the DfAM score for this part, the part was scored using both worksheets: (1) MEX and (2) LPBF. As shown in Table 2, the scoring approach for each method can be seen. As discussed previously in Section 3.1, all the features were scored throughout the part, and if a category consisted of multiple features of varying scores, the scores were averaged together. Due to the size of some features in this example design, each process results in largely the same score. The only differentiator in this case is for slanted surfaces; MEX machines can print them at a steeper angle than those printed with LPBF machines [44]. Because of this difference, the slanted surfaces for MEX score a 5, while the slanted surfaces for LPBF score a 3. The two cumulative DfAM scores are normalized before they are inserted into the build time estimation model, and from the DfAM score, the part is found to be slightly more viable for MEX.

Table 2. Part 000 Scoring Rubric for MEX and LPBF

Geometric Features											MEX	LPBF
Pins/Cylinders	5										5	5
Thin Walls	5	5									5	5
Slots/Grooves	5										5	5
Sharp Corners	2	2	2	2	2	1	2	2	1	1	1.7	1.7
Slanted Surfaces	5's for MEX, 3's for LPBF										5	3
Overhangs	1										1	1
Bridges	1										1	1
Internal Holes	1	1									1	1
Height/Width Ratio	5										5	5
Thick Sections	1										1	1
Escape Holes	5										5	5
Threaded Features	3										3	3
DfAM Score											0.645	0.612

4.1.2. Build Time and Material Usage of Case Study 1

To compare the values generated by the model, a ground truth needed to be determined to test the accuracy of the build time and volume estimation model. For MEX, a Prusa XL printer was selected to act as the printer, where PrusaSlicer acted as the required slicing software. Each part was sliced in the orientation that matched the drawing to remain consistent, and the values for build time and part volume were extracted from the slicer. The printer settings used in PrusaSlicer were: (1) supports set to everywhere, (2) a 0.4 mm nozzle diameter, and (3) a 0.2 mm layer height. For LPBF, an EOS M280 machine was selected as the printer, with the respective slicing software being Materialise Magics. Each part in the set was imported into Magics, orientated in the exact manner depicted in the drawing, and sliced with supports on. The build time, comprised of three categories: (1) part scan time, (2) support scan time and (3) recoat time, and material usage were all extracted from the slicer. The printer settings set in Magics were: (1) normal tree supports, (2) a 200W Yb-fiber laser, (3) a laser focus diameter of 100 microns, and (4) a recoat time of 8.8 seconds. For the case study, the relevant parameters for the build time estimation model can be seen in Table 4. The build rate, layer delay and support print speed for MEX were determined from the advanced settings found within the slicer, whereas the build rate and recoat time for the LPBF process were given by Simpson [33]. The laser type, laser focus diameter and layer height for LPBF were all selected from the EOS 280 datasheet [45].

Table 3. MEX and LPBF Estimation Parameters

AM Process	Dimension	Dimension Abbreviation	Value
MEX	Build Rate	\dot{V}_{ME}	15 mm ³ /s
	PLA Density	D_{PLA}	0.00124 g/mm ³
	Layer Height	h_{ME}	200 μ m
	Layer Delay	t_d	3 s
	Support Print Speed	v_s	110 mm/s
LPBF	Build Rate	\dot{V}_{LPBF}	9 mm ³ /s
	Ti-6Al-4V Density	D_{Ti}	0.0044 g/mm ³
	Layer Height	h_{LPBF}	60 μ m
	Laser Focus Diameter	d_{focus}	100 μ m
	Scan Speed	v_{ss}	7 m/s
	Recoat Time	t_R	8.8 s
	Laser Type	Yb-Fiber Laser	200 W

Alongside the estimated build time and material usage of the part, a ground truth needed to be established, which can be used to help determine the accuracy of the estimation approach. These ground truth values were established by using the built-in estimation tools in both PrusaSlicer and Magics. The CAD model for this part was not used during the scoring process; however, it is used here as a comparison tool. The actual time and material usage and estimated time and material usage for this part are compared in Table 4. Comparing the percent error, the percent error for time for MEX was 20.76%, whereas the percent error for material usage for MEX was 87.25%. For LPBF, the percent error for time was 8.67% and the percent error for material usage was 12.95%. Looking closer at the actual meaning of the percent errors, the time difference between the real time and estimated time was found to be 1.01 hrs. and 0.09 hrs. for MEX and LPBF, respectively. With this difference between estimators, the LPBF model better estimated the build time for this given part as well as the material usage for this part. Even though the DfAM score is higher for MEX than it is LPBF, indicating that this part is better suited for MEX, it does not directly impact how well the estimator anticipates the build time and material usage.

Table 4. Part 000 Build Time and Material Usage Comparison

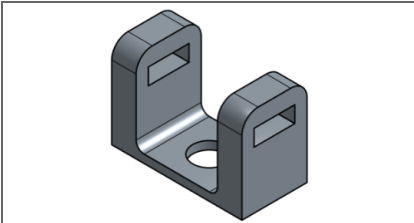
AM Process	Real Time [hrs.]	Estimated Time [hrs.]	Percent Error [%]	Time Error [hrs.]	Real Volume [mm ³]	Estimated Volume [mm ³]	Absolute Percent Error [%]
MEX	4.83	5.84	20.76	1.01	2.63 x 10 ⁵	1.41 x 10 ⁵	87.25
LPBF	6.45	6.36	8.67	0.09	3.10 x 10 ⁵	2.70 x 10 ⁵	12.95

Looking directly at the part and support scan time for this part, the LPBF model estimates a support scan time as 0.22 hrs. whereas the actual support scan time was found to be 0.54 hrs. The part scan time was estimated to be 2.60 hrs., and the actual part scan time was found to be 2.59 hrs. This small difference indicates that the model can accurately predict the scan time of this part well, as well as the support scan time.

4.2. Part ID 145

The second case study follows the scoring and estimation of the part denoted as 145. The part's dimensions and bounding box volume can be seen in Table 5, alongside its isometric view for illustrative purposes, similar to Case Study 1. Intuitively, this part appears better suited for AM when compared with Part 000, as this part's main downside is its two bridging features. The part was scored using each worksheet as well, and its scoring breakdown is discussed as follows.

Table 5. Part 145 Maximum Dimensions

	Drawing Dimensions	Value
	Maximum X [mm]	20.32
	Maximum Y [mm]	10.16
	Maximum Z [mm]	13.97
	Bounding Box Volume [mm ³]	1081.396

4.2.1. Scoring Rubric of Case Study 2

Again, the part was scored using the MEX and LPBF respective worksheets. Due to the size of the geometric features on part 145, it scored the same DfAM score for both processes. For some instances, DfAM scores for both MEX and LPBF processes can be the same due to how the

rubrics and designs interact. For example, LPBF has tighter accuracy, meaning the thresholds for scoring are based on smaller values [44]. If a feature dimension exceeds the threshold for MEX, it will almost certainly exceed it for LPBF as well, leading to identical scores. Additionally, some worksheet categories have the same thresholds for both processes, which naturally results in similar scores regardless of the process used. The part scored a normalized DfAM score of 0.80, which is expected, due to this part being generally better suited for AM over Part 000. Because each process scored the same, this part is equally viable for manufacturing for both processes, and the likelihood of a successful print are high. However, depending on the requirements for a given part, such as force and loading constraints, its application and functionality, one process may be recommended over another. The DfAM score helps determine the manufacturability, of a given part, but does not provide any insight of the suitability of the design for its intended purpose.

Table 6. Part 145 Scoring Rubric for MEX and LPBF

Geometric Features						MEX	LPBF	
Pins/Cylinders	5					5	5	
Thin Walls	5					5	5	
Slots/Grooves	3	3				3	3	
Sharp Corners	3	3	3	3	2	2	1.71	1.71
Slanted Surfaces	5					5	5	
Overhangs	5					5	5	
Bridges	2	2				2	2	
Internal Holes	1	1				1	1	
Height/Width Ratio	5					5	5	
Thick Sections	5					5	5	
Escape Holes	5					5	5	
Threaded Features	5					5	5	
DfAM Score						0.80	0.80	

4.2.2. Build Time and Material Usage of Case Study 2

Similarly to Case Study 1, the part was sliced in PrusaSlicer for MEX and Magics for LPBF to establish a ground truth alongside the estimated values. The actual time and material usage and estimated time and material usage for this part are compared in Table 7. Comparing the percent error, the percent error for time for MEX was 34.85%, whereas the percent error for material usage for MEX was 28.54%. For LPBF, the percent error for time was 19.25% and the percent error for material usage was 35.76%. Looking closer at the actual meaning of the percent errors, the time difference between the real time and estimated time was found to be 0.06 hrs. and 0.14 hrs., for MEX and LPBF, respectively. With this difference between estimators, the LPBF model better estimated the build time for this given part and the MEX model better estimated the material usage for this part. While the percentage error is higher for the MEX model, a difference of 0.06 hrs. is just 3.6 minutes. For the LPBF model, the difference of 0.14 hrs. is 8.4 minutes. This illustrated that percentage error depends not just on the size of the difference in time, but the significant difference in time is relative to the actual print time.

Table 7. Part 145 Build Time and Material Usage Comparison

AM Process	Real Time [hrs.]	Estimated Time [hrs.]	Percent Error [%]	Time Error [hrs.]	Real Volume [mm ³]	Estimated Volume [mm ³]	Absolute Percent Error [%]
MEX	0.18	0.12	34.85	0.06	9.19 x 10 ²	6.57 x 10 ²	28.54
LPBF	0.72	0.58	19.25	0.14	1.09 x 10 ³	6.99 x 10 ²	35.76

5. Conclusion and Future Work

This paper provides an initial framework for scoring and estimating the build time and material usage for AM designs, when only 2D drawing files may be available to use. The framework enables a user to evaluate the suitability of a provided part for AM using a feature-based DfAM score, which is used to estimate the build time and build volume, without the need for a CAD model. Considerations such as AM print process, material selection, DfAM score variation and printing-related variable were discussed using two case studies. The first case study involved a part that was intuitively believed to be not ideal for AM, due to its large geometric features hindering the build process, while the second case involved a part that was intuitively believed to be suitable for AM. Ultimately these case studies demonstrate that the approach shows potential in estimating build time and material usage for both LPBF and MEX processes but also illustrate the challenges that accompany each process. As an example, while the estimation process is automated, obtaining the DfAM score for each part requires a significant amount of AM expertise, along with many hours of engaged, hands-on involvement.

Although this work takes strides to guide users in properly scoring and printing parts intended for AM, some improvements can be made. The scoring process is heavily labor intensive and prone to inter-rater variability; due to the various ways evaluators can interpret the drawings. Refining the scoring criteria and automating the scoring process using machine learning is ideal, as it removes the need for any human evaluators and expedites insight into print feasibility. Additional design guidelines such as different geometric features will also be investigated once a larger dataset is evaluated. Beyond improving the quality of the scoring rubric, future work will focus on understanding the use of these AM models in an industry setting. There is a need for robust human-subjects experimentation with engineers and designers to identify the significant impacts that the use of this AM scoring worksheet and estimation model have on industry standards and practice.

6. Acknowledgement

This research was conducted through the support of the Naval Air Systems Command under Contract No. N6833525C0023. NAVAIR Public Release 2025-0363 Distribution Statement A - "Approved for public release; distribution is unlimited". Any opinions, findings, and conclusions expressed in this paper are solely the responsibility of the authors and do not necessarily represent the views of NAVAIR.

References

- [1] Costabile, G., Fera, M., Fruggiero, F., Lambiase, A., and Pham, D., 2017, "Cost Models of Additive Manufacturing: A Literature Review," *Int. J. Ind. Eng. Comput.*, pp. 263–283. <https://doi.org/10.5267/j.ijiec.2016.9.001>.
- [2] Campbell, I., Combrinck, J., De Beer, D., and Barnard, L., 2008, "Stereolithography Build Time Estimation Based on Volumetric Calculations," *Rapid Prototyp. J.*, 14(5), pp. 271–279. <https://doi.org/10.1108/13552540810907938>.
- [3] Esawi, A. M. K., and Ashby, M. F., 2003, "Cost Estimates to Guide Pre-Selection of Processes," *Mater. Des.*, 24(8), pp. 605–616. [https://doi.org/10.1016/S0261-3069\(03\)00136-5](https://doi.org/10.1016/S0261-3069(03)00136-5).

- [4] Mahadik, A., and Masel, D., 2018, “Implementation of Additive Manufacturing Cost Estimation Tool (AMCET) Using Break-down Approach,” *Procedia Manuf.*, 17, pp. 70–77. <https://doi.org/10.1016/j.promfg.2018.10.014>.
- [5] Booth, J. W., Alperovich, J., Chawla, P., Ma, J., Reid, T. N., and Ramani, K., 2017, “The Design for Additive Manufacturing Worksheet,” *J. Mech. Des.*, 139(100904). <https://doi.org/10.1115/1.4037251>.
- [6] Oropallo, W., and Piegl, L. A., 2016, “Ten Challenges in 3D Printing,” *Eng. Comput.*, 32(1), pp. 135–148. <https://doi.org/10.1007/s00366-015-0407-0>.
- [7] Alexander, P., Allen, S., and Dutta, D., 1998, “Part Orientation and Build Cost Determination in Layered Manufacturing,” *Comput.-Aided Des.*, 30(5), pp. 343–356. [https://doi.org/10.1016/S0010-4485\(97\)00083-3](https://doi.org/10.1016/S0010-4485(97)00083-3).
- [8] Zhang, Y., Bernard, A., Harik, R., and Karunakaran, K. P., 2017, “Build Orientation Optimization for Multi-Part Production in Additive Manufacturing,” *J. Intell. Manuf.*, 28(6), pp. 1393–1407. <https://doi.org/10.1007/s10845-015-1057-1>.
- [9] White, L., Liang, X., Zhang, G., Cagan, J., and Zhang, Y. J., 2024, “A Modified Simulated Annealing-Based Method for Hybrid Lattice Support Structure Design in LPBF Additive Manufacturing,” *J. Comput. Inf. Sci. Eng.*, 24(121002). <https://doi.org/10.1115/1.4066660>.
- [10] Schmelzle, J., Kline, E. V., Dickman, C. J., Reutzel, E. W., Jones, G., and Simpson, T. W., 2015, “(Re)Designing for Part Consolidation: Understanding the Challenges of Metal Additive Manufacturing,” *J. Mech. Des.*, 137(11), p. 111404. <https://doi.org/10.1115/1.4031156>.
- [11] Utley, E., 2017, “An Introduction to Designing for Metal 3D Printing,” *SOLIDWORKS Blog*. [Online]. Available: <https://blogs.solidworks.com/solidworksblog/2017/06/introduction-designing-metal-3d-printing.html>. [Accessed: 16-Apr-2025].
- [12] Herzog, D., Asami, K., Scholl, C., Ohle, C., Emmelmann, C., Sharma, A., Markovic, N., and Harris, A., 2022, “Design Guidelines for Laser Powder Bed Fusion in Inconel 718,” *J. Laser Appl.*, 34(1), p. 012015. <https://doi.org/10.2351/7.0000508>.
- [13] “Design Specifications for 3D Models (Form 4 Generation),” *Formlabs*. [Online]. Available: <http://support.formlabs.com/>. [Accessed: 25-Apr-2025].
- [14] “Origin_one_-_en_a4_design_guide.Pdf.” [Online]. Available: https://www.seido-systems.com/sites/seido_systems/files/uploads/media/files/origin_one_-_en_a4_design_guide.pdf. [Accessed: 14-Apr-2025].
- [15] “How to Design Parts for FDM 3D Printing,” *Protolabs Netw.* [Online]. Available: <https://www.hubs.com/knowledge-base/how-design-parts-fdm-3d-printing/>. [Accessed: 30-Mar-2025].
- [16] “Stereolithography SLA 3D Printing Design Guidelines | Additive Guides,” *Proto3000*. [Online]. Available: <https://proto3000.com/service/3d-printing-services/materials/overview/design-guidelines/sla-3d-printing-design-guidelines/>. [Accessed: 14-Apr-2025].
- [17] Bracken, J., Pomorski, T., Armstrong, C., Prabhu, R., Simpson, T. W., Jablow, K., Cleary, W., and Meisel, N. A., 2020, “Design for Metal Powder Bed Fusion: The Geometry for Additive Part Selection (GAPS) Worksheet,” *Addit. Manuf.*, 35, p. 101163. <https://doi.org/10.1016/j.addma.2020.101163>.
- [18] Yang, S., Page, T., Zhang, Y., and Zhao, Y. F., 2020, “Towards an Automated Decision Support System for the Identification of Additive Manufacturing Part Candidates,” *J. Intell. Manuf.*, 31(8), pp. 1917–1933. <https://doi.org/10.1007/s10845-020-01545-6>.

- [19] Li, Z., Zhang, Z., Shi, J., and Wu, D., 2019, “Prediction of Surface Roughness in Extrusion-Based Additive Manufacturing with Machine Learning,” *Robot. Comput.-Integr. Manuf.*, 57, pp. 488–495. <https://doi.org/10.1016/j.rcim.2019.01.004>.
- [20] Page, T. D., Yang, S., and Zhao, Y. F., 2019, “Automated Candidate Detection for Additive Manufacturing: A Framework Proposal,” *Proc. Des. Soc. Int. Conf. Eng. Des.*, 1(1), pp. 679–688. <https://doi.org/10.1017/dsi.2019.72>.
- [21] Chan, S. L., Lu, Y., and Wang, Y., 2018, “Data-Driven Cost Estimation for Additive Manufacturing in Cybermanufacturing,” *J. Manuf. Syst.*, 46, pp. 115–126. <https://doi.org/10.1016/j.jmsy.2017.12.001>.
- [22] Niazi, A., Dai, J. S., Balabani, S., and Seneviratne, L., 2005, “Product Cost Estimation: Technique Classification and Methodology Review,” *J. Manuf. Sci. Eng.*, 128(2), pp. 563–575. <https://doi.org/10.1115/1.2137750>.
- [23] Datta, P. P., and Roy, R., 2010, “Cost Modelling Techniques for Availability Type Service Support Contracts: A Literature Review and Empirical Study,” *CIRP J. Manuf. Sci. Technol.*, 3(2), pp. 142–157. <https://doi.org/10.1016/j.cirpj.2010.07.003>.
- [24] García-Crespo, Á., Ruiz-Mezcua, B., López-Cuadrado, J. L., and González-Carrasco, I., 2011, “A Review of Conventional and Knowledge Based Systems for Machining Price Quotation,” *J. Intell. Manuf.*, 22(6), pp. 823–841. <https://doi.org/10.1007/s10845-009-0335-1>.
- [25] Kadir, A. Z. A., Yusof, Y., and Wahab, M. S., 2020, “Additive Manufacturing Cost Estimation Models—a Classification Review,” *Int. J. Adv. Manuf. Technol.*, 107(9), pp. 4033–4053. <https://doi.org/10.1007/s00170-020-05262-5>.
- [26] Yim, S., and Rosen, D., 2012, “Build Time and Cost Models for Additive Manufacturing Process Selection,” *Volume 2: 32nd Computers and Information in Engineering Conference, Parts A and B*, American Society of Mechanical Engineers, Chicago, Illinois, USA, pp. 375–382. <https://doi.org/10.1115/DETC2012-70940>.
- [27] Ruffo, M., Tuck, C., and Hague, R., 2006, “Empirical Laser Sintering Time Estimator for Duraform PA,” *Int. J. Prod. Res.*, 44(23), pp. 5131–5146. <https://doi.org/10.1080/00207540600622522>.
- [28] Pham, D. T., and Wang, X., 2000, “Prediction and Reduction of Build Times for the Selective Laser Sintering Process,” *Proc. Inst. Mech. Eng. Part B*, 214(6), pp. 425–430. <https://doi.org/10.1243/0954405001517739>.
- [29] Taghian, M., Mosallanejad, M. H., Lannunziata, E., Del Greco, G., Iuliano, L., and Saboori, A., 2023, “Laser Powder Bed Fusion of Metallic Components: Latest Progress in Productivity, Quality, and Cost Perspectives,” *J. Mater. Res. Technol.*, 27, pp. 6484–6500. <https://doi.org/10.1016/j.jmrt.2023.11.049>.
- [30] Zhu, Z., Dhokia, V., and Newman, S. T., 2016, “A New Algorithm for Build Time Estimation for Fused Filament Fabrication Technologies,” *Proc. Inst. Mech. Eng. Part B J. Eng. Manuf.*, 230(12), pp. 2214–2228. <https://doi.org/10.1177/0954405416640661>.
- [31] Di Angelo, L., Di Stefano, P., and Guardiani, E., 2019, “A Build Time Estimator for Additive Manufacturing,” *2019 II Workshop on Metrology for Industry 4.0 and IoT (MetroInd4.0&IoT)*, pp. 344–349. <https://doi.org/10.1109/METROI4.2019.8792907>.
- [32] Di Angelo, L., Di Stefano, P., and Guardiani, E., 2020, “A Build-Time Estimator for Additive Manufactured Objects,” *Design Tools and Methods in Industrial Engineering*, C. Rizzi, A.O. Andrisano, F. Leali, F. Gherardini, F. Pini, and A. Vergnano, eds., Springer

- International Publishing, Cham, pp. 925–935. https://doi.org/10.1007/978-3-030-31154-4_79.
- [33] Simpson, T. W., 2020, “Industrializing AM: A Simple Cost Equation,” *Addit. Manuf. Media*. [Online]. Available: <https://www.additivemanufacturing.media/articles/industrializing-am-a-simple-cost-equation>. [Accessed: 03-Nov-2024].
- [34] “ABC: A Big CAD Model Dataset For Geometric Deep Learning : Faculty Digital Archive : NYU Libraries.” [Online]. Available: <https://archive.nyu.edu/handle/2451/43778>. [Accessed: 21-May-2025].
- [35] MakerVerse, 2024, “The Laser Powder Bed Fusion (L-PBF) Design Guide,” MakerVerse. [Online]. Available: <https://www.makerverse.com/resources/3d-printing/the-laser-powder-bed-fusion-l-pbf-design-guide/>. [Accessed: 14-Apr-2025].
- [36] Herzog, D., Asami, K., Scholl, C., Ohle, C., Emmelmann, C., Sharma, A., Markovic, N., and Harris, A., 2022, “Design Guidelines for Laser Powder Bed Fusion in Inconel 718,” *J. Laser Appl.*, 34(1), p. 012015. <https://doi.org/10.2351/7.0000508>.
- [37] Ramazani, H., and Kami, A., 2022, “Metal FDM, a New Extrusion-Based Additive Manufacturing Technology for Manufacturing of Metallic Parts: A Review,” *Prog. Addit. Manuf.*, 7(4), pp. 609–626. <https://doi.org/10.1007/s40964-021-00250-x>.
- [38] Selvakannan, PR., Mazur, M., and Sun, X., 2022, “Material Extrusion and Vat Photopolymerization—Principles, Opportunities and Challenges,” *Additive Manufacturing for Chemical Sciences and Engineering*, S.K. Bhargava, S. Ramakrishna, M. Brandt, and PR. Selvakannan, eds., Springer Nature, Singapore, pp. 53–76. https://doi.org/10.1007/978-981-19-2293-0_3.
- [39] “FDM 3D Printing Design Tips: Best Practices,” Xometry Pro. [Online]. Available: <https://xometry.pro/en/articles/fdm-design-tips/>. [Accessed: 30-Mar-2025].
- [40] “Design Rules & Best Practices for FFF 3D Printing,” Hydra Res. [Online]. Available: <https://www.hydraresearch3d.com/design-rules>. [Accessed: 14-Apr-2025].
- [41] “Can You Metal 3D Print Threaded Holes?,” Geomiq. [Online]. Available: <https://geomiq.com/blog/can-you-metal-3d-print-threaded-holes/>. [Accessed: 02-Oct-2024].
- [42] Farzadi, A., Waran, V., Solati-Hashjin, M., Rahman, Z. A. A., Asadi, M., and Osman, N. A. A., 2015, “Effect of Layer Printing Delay on Mechanical Properties and Dimensional Accuracy of 3D Printed Porous Prototypes in Bone Tissue Engineering,” *Ceram. Int.*, 41(7), pp. 8320–8330. <https://doi.org/10.1016/j.ceramint.2015.03.004>.
- [43] “Wohlers Report 2019,” Wohlers Assoc. [Online]. Available: <https://wohlersassociates.com/product/wohlers-report-2019/>. [Accessed: 13-May-2025].
- [44] Klahn, C., and Leutenecker-Twelsiek, B., 2023, “Design Guidelines,” *Springer Handbook of Additive Manufacturing*, E. Pei, A. Bernard, D. Gu, C. Klahn, M. Monzón, M. Petersen, and T. Sun, eds., Springer International Publishing, Cham, pp. 177–198. https://doi.org/10.1007/978-3-031-20752-5_12.
- [45] “EOS M280 DMLS Metal 3D Printer | NJIT Makerspace.” [Online]. Available: <https://www.njitmakerspace.com/equipment/eos-m280-dmls-metal-3d-printer>. [Accessed: 20-May-2025].